

## Observation of Condensed Phases of Quasiplanar Core-Softened Colloids

N. Osterman,<sup>1</sup> D. Babič,<sup>1</sup> I. Poberaj,<sup>1</sup> J. Dobnikar,<sup>2</sup> and P. Ziherl<sup>1,2</sup>

<sup>1</sup>*Department of Physics, University of Ljubljana, Jadranska 19, SI-1000 Ljubljana, Slovenia*

<sup>2</sup>*Jožef Stefan Institute, Jamova 39, SI-1000 Ljubljana, Slovenia*

(Received 25 July 2007; published 11 December 2007)

We experimentally study the condensed phases of repelling core-softened spheres in two dimensions. The dipolar pair repulsion between superparamagnetic spheres trapped in a thin cell is induced by a transverse magnetic field and softened by suitably adjusting the cell thickness. We scan a broad density range and we materialize a large part of the theoretically predicted phases in systems of core-softened particles, including expanded and close-packed hexagonal, square, chainlike, stripe or labyrinthine, and honeycomb phase. Further insight into their structure is provided by Monte Carlo simulations.

DOI: [10.1103/PhysRevLett.99.248301](https://doi.org/10.1103/PhysRevLett.99.248301)

PACS numbers: 82.70.Dd, 64.60.Cn, 64.70.Kb

One of the ageless challenges of material science is to engineer structure formation. Recently, of particular interest are the various crystalline phases of colloidal particles [1] which may be used for self-assembled nanomaterials [2], photonic crystals [3], macroporous polymer membranes [4], biochemical applications [5], etc. In this context, it is imperative to understand the link between the interparticle potential and the phase behavior of the ensemble. Experimentally, this link can be studied readily using tabletop equipment which provides the full microscopic real-time structural information, wherefrom the subtle relations between the microscopic and the macroscopic properties of the system can be reconstructed. Complementary insight can be obtained by inverse methodology to identify the optimal pair potential that produces a given target structure [6].

A basic limitation of these efforts is the spherical shape typical for many colloids and the ensuing isotropy of the interparticle potential. This is the main reason why the most common ordered structures are close packed, i.e., the hexagonal and the face-centered cubic lattice [7,8] in two and three dimensions, respectively. A richer phase diagram can be induced by anisotropic interactions due to, e.g., surface treatment of particles [9], external fields [10], or a liquid-crystalline solvent [11]. Another route to the more open lattices is isotropic pair interactions with a radial profile characterized by two length scales, such as the combination of hard-core and penetrable-sphere repulsion [12]. If the shoulder/core diameter ratio exceeds about 2, this pair potential stabilizes a range of mesophases intervening between the fluid and the close-packed crystal. In two dimensions, the theoretical phase sequence includes loose- and close-packed hexagonal lattice, monomer, dimer, and trimer fluids, stripe and labyrinthine phases, honeycomb lattice, etc. [12–14]. Very similar behavior has been predicted numerically in paramagnetic particles confined to a plane and interacting with a dipolar repulsion induced by a transverse magnetic field and softened by a Lennard-Jones interaction [15]. For large shoulder/core diameter ratios, the set of mesophases reduces to micellar, lamellar, and inverted micellar structure [16].

The theoretical insight into the mesophases formed by particles with a core-softened isotropic repulsive pair potential in two dimensions is reasonably comprehensive, but the physical evidence of their stability is still lacking. In this Letter, we study the phase sequence of such a system experimentally using superparamagnetic spheres, tailoring the profile of interaction with external magnetic field and spatial constraints. We discover a host of the predicted structures, and we corroborate the observations by numerical simulations.

We used a thin wedge-shaped cell formed by nearly parallel glass plates and filled by a water solution of 1.05  $\mu\text{m}$  superparamagnetic spheres (Dynabeads, MyOne Carboxy). A small (5 mg/ml) amount of sodium dodecyl sulfate was added to suppress the van der Waals interactions and prevent sticking of the colloids. As in related experiments [17–22] the interparticle repulsion was induced by external magnetic field. The experimental setup is comprised of a laser tweezers system built around an inverted optical microscope (Zeiss Axiovert 200M) and a cw diode pumped Nd:YAG laser (Coherent, Compass 2500MN), and equipped with three orthogonal pairs of Helmholtz coils driven by a computer-controlled current source. Multiple laser traps used to manipulate the spheres are created by time-sharing using acousto-optic deflectors (IntraAction, DTD-274HA6) driven by a beam-steering controller (Aresis, Tweez). The cell is illuminated with a halogen lamp, and the micrographs are recorded in the bright field with a fast complementary metal oxide semiconductor camera (PixeLINK, PL-A741). Image analysis is performed off-line with custom-made particle tracking software.

The key feature of the system which softens the repulsion between the induced magnetic dipoles of the spheres is the cell thickness: If it is somewhat larger than the sphere diameter, the centers of two nearby spheres are not restricted to a plane perpendicular to the magnetic field. This makes their interaction at small separations less repulsive compared to spheres lying in the plane (or even attractive). The pair potential is

$$U(r, z) = K \frac{r^2 - 2z^2}{(r^2 + z^2)^{5/2}}, \quad (1)$$

where  $K = \pi\sigma^6\chi^2 B^2/144\mu_0$  is the interaction constant which depends on the magnetic induction  $B$  and the magnetic susceptibility  $\chi$  of the particles,  $r$  and  $z$  are the in-plane and the vertical separations of the spheres, respectively, and  $\sigma$  is their diameter (Fig. 1). It is convenient to write the cell thickness as  $\sigma + h$ : Thus  $h$  measures the deviation from a truly planar system. In the thin part of the cell where  $h \rightarrow 0$ ,  $U$  reduces to  $K/r^3$ , whereas for  $h > 0$  the repulsion is reduced at small distances by the relative vertical shift of the spheres. The in-plane interparticle force is  $F_r = -\partial U/\partial r = -3Kr(4z^2 - r^2)/(r^2 + z^2)^{7/2}$ . For spheres in contact in a cell of thickness  $\sigma + h < 2\sigma$ ,  $F_r = -3K\sqrt{\sigma^2 - h^2}(5h^2 - \sigma^2)/\sigma^7$  which is attractive for  $h > h_m = \sigma/\sqrt{5} \approx 0.447\sigma$ . The softening of the repulsion is most pronounced at cell thicknesses somewhat smaller than  $\sigma + h_m$ .

To verify that the in-plane pair interaction between the spheres is indeed described by the above law, we measured it using two isolated spheres, one attached to the lower glass plate and the other one (probe) confined laterally by a weak optical trap and pushed against the upper plate by the light pressure so that their vertical separation was fixed to  $h$ . The probe was repeatedly slowly dragged back and forth from the fixed sphere, and its trajectories were recorded and averaged to accurately determine the displacement of the probe particle from the trap center as a function of interparticle distance. To calculate the magnetic force on

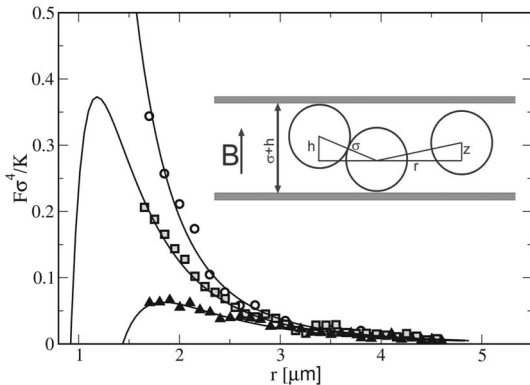


FIG. 1. Measured variability of the in-plane pair force profiles:  $r^{-4}$  repulsion (thin cell,  $h \ll h_m$ ; circles), softened repulsion ( $h \approx h_m$ ; squares), and oversoftened interaction (thick cell,  $h > h_m$ ; triangles) with the attractive part at small separations. For  $h = h_m$ , the in-plane hard-core diameter of the spheres is  $\approx 0.89 \mu\text{m}$ . The small-separation part of the force profile is not accessible with our method as the laser would act on both spheres, rendering the measurement impossible. In our experiment,  $B$  is typically around 10 mT and the induced pair forces are of the order of 0.1 pN at separations comparable to sphere diameter. Solid lines are theoretical fits for  $h = 0$ ,  $h = 0.46 \mu\text{m}$ , and  $h = 0.72 \mu\text{m}$ , respectively. Inset: experimental geometry in cross section.

the probe from the displacement profile, the stiffness of the laser potential was determined by analyzing the Brownian motion of the probe sphere with the magnetic field turned off. The procedure was repeated at a range of cell thicknesses and the three representative force profiles shown in Fig. 1 demonstrate that the system behaves as expected.

Having confirmed that the pair potential is given by Eq. (1), we studied the phase behavior of the system across a broad density range. We filled the cell with a dense suspension of spheres, and we first located the measuring site with cell thickness of about  $\sigma + h_m$ . As the cell thickness cannot be measured directly, we used the following protocol. In absence of the magnetic field, we herded the spheres at a given location into contact such that they formed clusters. We then turned on the field which caused the clusters to disintegrate. In the thick part of the cell where the potential was attractive at small separations the cluster disintegration was partial, whereas in the thin part with purely repulsive interactions the clusters disintegrated completely. By scanning the cell we identified the site with the desired thickness.

At this site, we increased the sphere density  $n$  in the part of the cell covered by the camera's field of view using the laser tweezers operating at high power to locally heat the suspension. The heating induced a hydrodynamic flow which dragged a large number of spheres toward the trap, thereby increasing the local sphere density almost to close packing. Then the laser was turned off which stopped the flow, and the magnetic field was turned on. The high-density region underwent an adiabatic expansion such that the system could be studied at decreasingly lower colloidal densities. A sizable change of the density took place on a time scale of about 10 s. This is much longer than the typical diffusion time of particles ( $< 10$  ms) [23] so that the expansion was slow enough to ensure quasiequilibrium at all times [24], and the hydrodynamic interactions due to expansion  $\sim 10^{-3}k_B T$  are negligible compared to the magnetic repulsion. The main advantage of this protocol is that it allows one to study the states of a fixed ensemble of over  $10^4$  spheres at the same location in the cell (and thus at the same cell thickness) across a range of densities. This excludes any deviations in the sample that could affect its behavior in an uncontrolled way and ensures that the phase transitions are induced solely by density variation.

Micrographs of the most interesting phases observed at various 2D volume fractions  $\eta = \pi\sigma^2 n/4$  shown in Fig. 2 include (i) fluid phase ( $\eta = 0.01$ ), (ii) expanded hexagonal lattice ( $\eta = 0.12$ ), (iii) coexisting expanded hexagonal and square lattice ( $\eta = 0.23$ ), (iv) coexisting expanded square lattice and chain phase ( $\eta = 0.31$ ), (v) chain phase with locally aligned finite-length strings ( $\eta = 0.34$ ), (vi) stripe or labyrinthine structure formed predominantly by a single cluster of interlaced strings of touching spheres ( $\eta = 0.39$ ), and (vii) coexisting honeycomb and dense square lattice at a high volume fraction ( $\eta = 0.54$ ). The square lattice observed at large  $\eta$  is consistent with the studies of

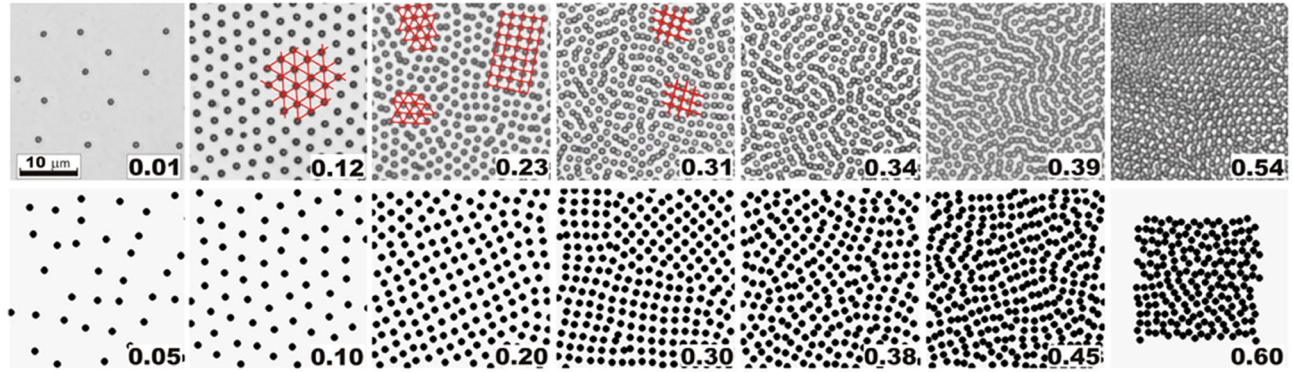


FIG. 2 (color online). Micrographs of the representative mesophases induced by varying the density (top row;  $B = 12.5$  mT which gives  $k \approx 400$ ) and the simulation snapshots (bottom row) labeled by the corresponding 2D volume fractions of colloids. Because of optical image distortion, the colloids on the micrographs appear slightly larger than their true size; in some of the micrographs, patches of the underlying lattices are emphasized to guide the eye. The reduced interaction strength of  $k = 375$  was used in simulations at all but the largest two volume fractions where  $k$  was set to 125 to improve convergence; the number of particles  $N = 1000$  except at  $\eta = 0.60$ , where  $N = 200$ .

packing of spheres in a wedge cell [25,26] where confinement stabilizes hexagonal, square, and prismatic lattices depending on the cell thickness. The agreement is understandable since at large densities, the dipolar magnetic repulsion is subdominant compared to the hard-core interaction: In Refs. [25,26] the square lattice was found to be the closest packing at thicknesses between  $\sigma$  and  $1.8\sigma$  which supports our data.

The observed mesophases are remarkably close to those found in the numerical simulations reported in Ref. [15] although the pair interaction is not exactly the same; a much more idealized hard-core–soft-shoulder interaction also gives a similar phase sequence [12,14]. This suggests that the mechanisms at work as well as the structures they produce are rather robust. Nonetheless, our system is not perfectly two dimensional, and the vertical position of a sphere is a restricted variable which does affect the symmetry of the in-plane equilibrium configuration. To understand the phase sequence in more detail, we performed 3D Monte Carlo simulations of up to 1000 spheres with the dipole-dipole pair repulsion in a cell of thickness  $\sigma + h_m$ . We varied the volume fraction and we focused on the low temperature limit corresponding to large reduced interaction strengths  $k = K/k_B T \sigma^3$ ; in the experiment,  $k \approx 400$ . We used periodic boundary conditions in several simulation box geometries; after reaching equilibrium (typically in a few million steps)  $50 \times 10^6$  averaging steps were performed to evaluate the energy per particle, the radial distribution function, and the static structure factor. The selected simulation snapshots in Fig. 2 are chosen to best reproduce the phase sequence seen in the micrographs. The agreement is very good, which also demonstrates that any effect of polydispersity of the superparamagnetic spheres used is unimportant.

The insight provided by the simulations goes beyond the experimental micrographs: It includes the spheres' vertical positions, which are uncorrelated and evenly distributed

across the available range as long as the volume fraction does not exceed about 0.05. However, for  $\eta \geq 0.1$  the distribution is bimodal with pronounced peaks corresponding to spheres touching the bottom and the top plate, and the system resembles an off-lattice two-state spin ensemble with dominant nearest-neighbor antiferromagnetic interaction. This interaction is frustrated by the hexagonal lattice, but the stripe, honeycomb, and square lattice with 2, 3, and 4 regularly arranged nearest neighbors, respectively, are compatible with alternating up-down positions of spheres. We computed the energies of the stripe, the square, and the hexagonal phase by fixing their in-plane structure [27]. The ground states of the nonfrustrated phases, such as the checkerboard square lattice, are ordered and unique, and their energies were calculated using a lattice sum, whereas the energy of the hexagonal lattice was evaluated numeri-

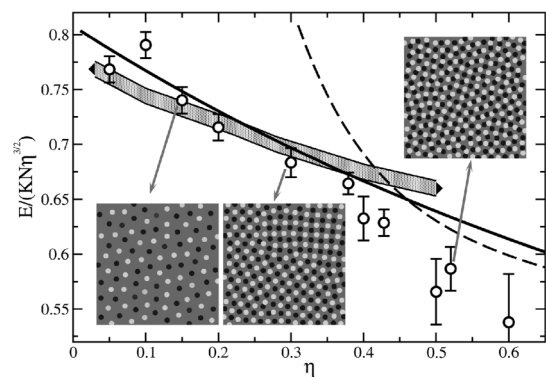


FIG. 3. Energy per particle of the ground states of hexagonal (broad shaded line; the line thickness represents the numerical inaccuracy), square (solid line), and stripe phases (dashed line) compared to the energies obtained by the Monte Carlo simulation (open circles with error bars). Also shown are the snapshots for  $\eta = 0.10$  (hexagonal lattice),  $\eta = 0.30$  (square lattice), and  $\eta = 0.52$  (labyrinthine structure) where the spheres' vertical positions are encoded by shades of gray.

cally in systems of up to 5000 spheres by annealing their vertical positions.

The results are shown in Fig. 3: At small  $\eta$ , the hexagonal phase has the lowest energy per particle among the three candidate phases, the square phase is stable at intermediate volume fractions, and at the highest volume fractions considered here the stripe phase is the stable configuration. In Fig. 3, we also plotted the energies of the equilibrium states obtained by the full Monte Carlo analysis that produced the snapshots shown in Fig. 2. Up to  $\eta \approx 0.4$ , the agreement of the energies calculated using lattice sums and simulations, respectively, is quite good. In this regime, the simulations as well as the experiments usually produce coexistence of the hexagonal and the square lattice rather than a pure lattice (Fig. 2). This can be understood based on the lattice sum results which predict a very similar dependence of the energies of the two lattices on  $\eta$ , and thus the coexistence regime obtained by Maxwell construction should extend over a broad density range. At volume fractions beyond  $\approx 0.4$ , the difference between the energies of the model structures and those obtained by simulations slightly exceeds the error bar of the latter suggesting that the stripe phase with perfectly parallel straight stripes is probably not the ground state and that the many turns and junctions may be an equilibrium feature of the system.

In conclusion, we report an experimental study where a core-softened repulsive interaction was induced in micrometer-size colloidal particles using the external magnetic field and fine-tuned by controlling the spatial constraints. Depending on the density, the system forms several self-assembled mesophases—the square, hexagonal, and honeycomb lattices as well as the labyrinthine structure—thereby experimentally validating the theoretical predictions pertaining to similar pair interactions [12,14,15]. The observed two-dimensional structures could be used for the fabrication of templates to promote the growth of colloidal crystals [28,29].

We thank J. Kotar for setting up the magnetic system, H. H. von Grünberg for stimulating discussions, and B. Kavčič for technical assistance. This work was supported by EC (Grant No. MERG-031089) and by Slovenian Research Agency (Grants No. J1-6502 and No. P1-0055).

- 
- [1] Y. Xia, B. Gates, Y. Yin, and Y. Lu, *Adv. Mater.* **12**, 693 (2000).
  - [2] J. H. Fendler, *Chem. Mater.* **8**, 1616 (1996).
  - [3] K. Busch and S. John, *Phys. Rev. E* **58**, 3896 (1998).
  - [4] P. Jiang, K. S. Hwang, D. M. Mittleman, J. F. Bertone, and V. L. Colvin, *J. Am. Chem. Soc.* **121**, 11 630 (1999).
  - [5] H. Kawaguchi, *Prog. Polym. Sci.* **25**, 1171 (2000).
  - [6] M. C. Rechtsman, F. H. Stillinger, and S. Torquato, *Phys. Rev. Lett.* **95**, 228301 (2005).
  - [7] K. Kremer, M. O. Robbins, and G. S. Grest, *Phys. Rev. Lett.* **57**, 2694 (1986).
  - [8] S. C. Mau and D. A. Huse, *Phys. Rev. E* **59**, 4396 (1999).

- [9] D. R. Nelson, *Nano Lett.* **2**, 1125 (2002).
- [10] A. Yethiraj and A. van Blaaderen, *Nature (London)* **421**, 513 (2003).
- [11] H. Stark, *Phys. Rep.* **351**, 387 (2001).
- [12] G. Malescio and G. Pellicane, *Nat. Mater.* **2**, 97 (2003).
- [13] Y. Norizoe and T. Kawakatsu, *Europhys. Lett.* **72**, 583 (2005).
- [14] E. A. Jagla, *J. Chem. Phys.* **110**, 451 (1999).
- [15] P. J. Camp, *Phys. Rev. E* **68**, 061506 (2003).
- [16] M. Glaser, G. M. Grason, R. D. Kamien, A. Košmrlj, C. D. Santangelo, and P. Zihlerl, *Europhys. Lett.* **78**, 46004 (2007).
- [17] K. Zahn, R. Lenke, and G. Maret, *Phys. Rev. Lett.* **82**, 2721 (1999).
- [18] K. Zahn and G. Maret, *Phys. Rev. Lett.* **85**, 3656 (2000).
- [19] R. Bubeck, C. Bechinger, S. Naser, and P. Leiderer, *Phys. Rev. Lett.* **82**, 3364 (1999).
- [20] W. Wen, L. Zhang, and P. Sheng, *Phys. Rev. Lett.* **85**, 5464 (2000).
- [21] C. Eisenmann, U. Gasser, P. Keim, and G. Maret, *Phys. Rev. Lett.* **93**, 105702 (2004).
- [22] A. Erbe and L. Baraban (private communication).
- [23] In equilibrium, a thermally excited particle in the potential well formed by its neighbors fluctuates around its mean position by about  $d \sim [k_B T \sigma^5 f(\eta)/384K]^{1/2}$ , where  $f(\eta)$  is a numerical factor which equals 1 at close packing and  $\sim 1000$  at  $\eta \approx 0.1$ . The typical time needed to traverse this distance is  $\tau \sim d^2/D$ , where  $D = k_B T/3\pi\nu\sigma$  is the diffusion constant;  $\nu$  is the viscosity. In our case,  $\tau \sim 10 \mu\text{s}$  at  $\eta = 0.5$  and  $\tau \sim 10 \text{ ms}$  at  $\eta = 0.1$ .
- [24] Typically, the system consists of several domains whose size increases with decreasing density simultaneously with the deceleration of the expansion rate (Fig. 2). Domain coarsening is slow at large densities, whereas at  $\eta \lesssim 0.3$  it is faster than the structural transformations induced by expansion. Nonetheless, we are convinced that the intradomain structure at a given  $\eta$  does correspond to the equilibrium configuration of the colloids. This was verified by additional static experiments at  $\eta = 0.31$  where square symmetry is expected (Fig. 2). The initial zero-field configuration of the colloids in the sealed cell was liquid-like, and after the magnetic field was turned on and the system was left to equilibrate for extended periods of time we observed square domains much larger than those seen in quasistatic experiments.
- [25] P. Pieranski, L. Strzelecki, and B. Pansu, *Phys. Rev. Lett.* **50**, 900 (1983).
- [26] S. Naser, C. Bechinger, P. Leiderer, and T. Palberg, *Phys. Rev. Lett.* **79**, 2348 (1997).
- [27] We analyzed all stripe structures of width 1 by varying the intrastripe separation, the stripe spacing, and the staggering of neighboring stripes. At any given volume fraction, the minimal-energy configuration consists of close-packed stripes, and the neighboring stripes are out of registry by 1 sphere diameter such that the stripe structure resembles a square lattice compressed along one lattice vector and stretched along the other one as much as possible.
- [28] A. van Blaaderen, R. Ruel, and P. Wiltzius, *Nature (London)* **385**, 321 (1997).
- [29] K. H. Lin, J. C. Crocker, V. Prasad, A. Schofield, D. A. Weitz, T. C. Lubensky, and A. G. Yodh, *Phys. Rev. Lett.* **85**, 1770 (2000).